MolecularMedicine

Supplemental Data

Signatures of miR-181a on the Renal Transcriptome and Blood Pressure

Francine Z Marques,[1] Simon PR Romaine,[2] Matthew Denniff,[2] James Eales,[2] John Dormer,[3] Ingrid M Garrelds,[4] Lukasz Wojnar,[5] Katarzyna Musialik,[6] Barbara Duda-Raszewska,[7] Bartlomiej Kiszka,[7] Magdalena Duda,[7] Brian J Morris,[8] Nilesh J Samani,[2,9] AH Jan Danser,[4] Pawel Bogdanski,[6] Ewa Zukowska-Szczechowska,[7] Fadi J Charchar,[1] and Maciej Tomaszewski[2,10]

Online address: http://www.molmed.org

The Feinstein Institute for Medical Research
Empowering Imagination. Pioneering Discovery.®
North Shore LIJ

SUPPLEMENTARY METHODS

Subjects

Human kidney samples were collected during the TRANScriptome of renaL humAn TissuE (TRANSLATE) Study (1). In brief, samples were obtained after surgery in 200 patients who underwent elective unilateral nephrectomy because of non-invasive renal cancer in one of three nephrology-urology centres [Silesian Renal Tissue Bank (2, 3), TRANSLATE P (recruitment conducted in Western Poland) and TRANSLATE Z (recruitment conducted in Southern Poland) (1)]. Each subject underwent standardized clinical phenotyping, including personal history (through anonymous coded questionnaires), anthropometry (i.e. weight, height) and triplicate measurements of blood pressure (BP) using a mercury sphygmomanometer (in a subset of samples – Silesian Renal Tissue Bank) (2, 3) or automatic digital BP monitoring (in the rest of the patients). Hypertension was diagnosed based on the criteria used previously (4, 5). All individuals were of white-European ancestry.

Serum samples from 200 subjects recruited in the Genetic Regulation of Arterial Pressure of Humans In the Community (GRAPHIC) Study were obtained for the replication experiment. Details of recruitment and phenotyping of GRAPHIC are described elsewhere (6, 7). Briefly, 520 nuclear families of white-European ancestry, with both parents aged 40–60 years and two adult offspring aged ≥ 18 years were identified through general practice records in Leicestershire, UK. All subjects (n = 2,037) were extensively phenotyped including both clinic BP (calculated as a mean of the second and third of three readings) and 24-h ambulatory BP (7). The subset of 199 subjects obtained for the present replication cohort were selected from the parental generation of the GRAPHIC cohort (n = 1,032) after the following initial exclusions: poor quality phenotype or genotype data (n = 9); on antihypertensive or lipid-lowering medication (n = 150); serum sample missing (n = 30) or low volume (n = 4). Following these exclusions, from amongst eligible subjects, 200 were selected on the basis of sex and extremes of mean 24-h ambulatory systolic BP. Thus, 100 men with the 50 highest and lowest values for mean 24-h ambulatory systolic BP were included in the replication sample, along with 100 women using the same criteria. One subject was further excluded due to a failure of RNA extraction leaving 199 included in the statistical analyses. No patients were receiving heparin and just six were receiving antiplatelet therapy.

All subjects gave written informed consent and the studies were approved by ethics committees at each institution.

Renal Tissue, Serum Processing and RNA Extraction

The renal tissue samples in the TRANSLATE Study were collected immediately after nephrectomy from a healthy (unaffected by cancer) pole of the kidney and immersed in RNA*later* (Life Technologies) before storage at –80°C, as previously described (1-3, 8). RNA was extracted from all kidney tissues using the miRNeasy kit (Qiagen) and stored at –80°C. RNA was also extracted from 100 μl (TRANSLATE) or 200 μl (GRAPHIC) of serum (secured from blood collected during recruitment and stored at –80°C) using the miRNeasy Serum/Plasma kit (Qiagen) from matching subjects. No pooling of samples was performed.

Quantitative Real-time PCR (qPCR)

The first-strand complementary synthesis reaction (cDNA) was performed using the High Capacity Reverse Transcriptase cDNA Synthesis kit (Life Technologies) for mRNA and the TaqMan® MicroRNA Reverse Transcription kit (Life Technologies) for miRNAs. Amplification reactions used the TaqMan® Fast Advanced Master Mix (Life Technologies) in a Viia7™ qPCR system (Life Technologies). TaqMan® assays were used to measure mRNA and miRNA expression (Supplemental Table S1) following the cycling conditions recommended by the supplier. β-actin (*ACTB*) mRNA

Supplementary Table S1. TaqMan® assays used to measure mRNA and microRNA expression.

Official symbol	TaqMan assay ID	Tissue	Comments	Study
ACTB (NM_001101)	Hs01060665_g1	Kidney	Housekeeping gene	TRANSLATE
REN (NM_000537.3)	Hs00982555_m1	Kidney	Renin mRNA	TRANSLATE
RNU6	1973	Kidney	Housekeeping gene	TRANSLATE
cel-miR-39	0200	Serum	Spike-in control	TRANSLATE, GRAPHIC
hsa-miR-181a	0480	Kidney/Serum	microRNA	TRANSLATE, GRAPHIC

Supplementary Table S2. Locked nucleic acid (LNA) probes used for *in situ* hybridization of microRNA staining.

miRNA/ Probe name	Details	Antiparallel sequence	RNA Tm	%LNA	Concentration
miR-181a	miRNA of interest	ACTCACCGACAGCGTTGAATGTT	85	23	50 nM
miR-126	Positive control	CATTATTACTCACGGTACGA	84	20	20 nM
Scramble	Negative control	TGTAACACGTCTATACGCCCA	87	21	20 nM

Tm, melting temperature.

Supplementary Table S3. Clinical characteristics of individuals in the TRANScriptome of renaL humAn TissuE (TRANSLATE) Study, displayed per recruitment centre.

Variable	SRTB	TRANSLATE P	TRANSLATE Z
N	67	80	53
Age (years)	58.9 (11.3)	63.1 (10.0)	62.9 (10.1)
BMI (kg/m^2)	27.7 (4.3)	27.4 (4.3)	27.9 (4.1)
Male sex	37 (55.2%)	52 (65.0%)	31 (58.5%)
SBP (mmHg)	134.4 (12.1)	142.6 (12.9)	129.1 (11.3)
DBP (mmHg)	82.0 (7.8)	88.2 (6.7)	75.6 (6.9)
Hypertension	43 (64.2%)	55 (68.8%)	36 (67.9)
Antihypertensive treatment	40 (59.7%)	39 (48.8%)	35 (66.0%)

Data are shown as means and standard deviations or numbers and percentages.
N, number of individuals; SRTB, Silesian Renal Tissue Bank; BMI, body mass index; SBP, systolic blood pressure; DBP, diastolic blood pressure.

was used as an internal reference transcript for renal mRNA expression and RNA U6 small nuclear 2 (*RNU6B*) for miRNA expression in the kidney; both were chosen based on previously published data. (8) In serum, the spike-in cel-miR-39 was used to normalize experimental variability in miRNA levels, in agreement with previously published studies (9-12). All expression experiments were run in duplicate (TRANSLATE) or triplicate (GRAPHIC). The delta cycle threshold (dCt), derived from normalization of mRNA and miRNAs to reference mRNAs, was used as qPCR measure of renal expression (13). dCt is an inverse measure of mRNA expression – the higher the value, the lower the abundance of the target examined in the tissue.

Renal *In Situ* Hybridization (ISH) and Immunohistochemistry

Formalin-fixed and paraffin-embedded (FFPE) kidney samples from a TRANSLATE individual were used to localize the expression of miR-181a (by ISH) and renin (by immunohistochemistry). ISH was performed using locked nucleic acid (LNA) probes (Exiqon, 20-50 nM) for miR-181a, positive control miRNA (miR-126) and a scrambled (negative control) probe (Supplemental Table S2), as described previously (13). Immunohistochemistry was performed using a renin mouse monoclonal antibody (clone 7D3-E3 at 2.5 μg/ml, ab134783, Abcam), followed by staining with EnVision+System-HRP (Dako). In immunohistochemistry images, the posi-

Supplementary Table S4. Basic demographic characteristics of TCGA individuals included in next-generation RNA-sequencing analysis of renal transcriptomes.

Phenotype	Values
N	69
Age (years)	63.0±12.0
Male sex	50 (72%)

Data are means and standard deviations or counts and percentages.

Supplementary Table S5. Association between blood pressure and the expression of renin mRNA in the kidney.

	Systolic blood pressure	Diastolic blood pressure
Kidney renin mRNA (dCt)	0.03±0.37	0.18±0.47
	NS	NS

Data are expressed as β-coefficients (with standard errors) from linear regression models in which blood pressure (BP) was the dependent variable and delta cycle thresholds (dCt) (inverse measure of renin mRNA expression) as one of the independent variables. NS, not statistically significant.

Supplementary Table S6. Pathways associated with renal expression of miR-181a – gene-set enrichment analysis of TCGA kidney transcriptomes characterized by next-generation RNA-sequencing.

Network label	Pathway database and name	Up- or down-regulated	FDR q-value	Genes in pathway	URL
B1	BioCarta complement pathway	Up	0.0074	16	http://www.broadinstitute.org/gsea/msigdb/cards/BIOCARTA_COMP_PATHWAY
B2	BioCarta CSK pathway	Up	0.001	20	http://www.broadinstitute.org/gsea/msigdb/cards/BIOCARTA_CSK_PATHWAY
B3	BioCarta NKT pathway	Up	<0.0001	18	http://www.broadinstitute.org/gsea/msigdb/cards/BIOCARTA_NKT_PATHWAY
K1	KEGG arginine and proline metabolism	down	0.0037	50	http://www.broadinstitute.org/gsea/msigdb/cards/KEGG_ARGININE_AND_PROLINE_METABOLISM
K2	KEGG oxidative phosphorylation	down	<0.0001	111	http://www.broadinstitute.org/gsea/msigdb/cards/KEGG_OXIDATIVE_PHOSPHORYLATION
K3	KEGG peroxisome	down	0.0005	75	http://www.broadinstitute.org/gsea/msigdb/cards/KEGG_PEROXISOME
K4	KEGG allograft rejection	Up	0.001	24	http://www.broadinstitute.org/gsea/msigdb/cards/KEGG_ALLOGRAFT_REJECTION
K5	KEGG antigen processing and presentation	Up	0.0074	54	http://www.broadinstitute.org/gsea/msigdb/cards/KEGG_ANTIGEN_PROCESSING_AND_PRESENTATION
K6	KEGG asthma	Up	0.001	17	http://www.broadinstitute.org/gsea/msigdb/cards/KEGG_ASTHMA
K7	KEGG autoimmune thyroid disease	Up	0.0041	25	http://www.broadinstitute.org/gsea/msigdb/cards/KEGG_AUTOIMMUNE_THYROID_DISEASE
K8	KEGG cell adhesion molecules CAMs	Up	0.0002	112	http://www.broadinstitute.org/gsea/msigdb/cards/KEGG_CELL_ADHESION_MOLECULES_CAMS
K9	KEGG chemokine signaling pathway	Up	0.0021	158	http://www.broadinstitute.org/gsea/msigdb/cards/KEGG_CHEMOKINE_SIGNALING_PATHWAY
K10	KEGG cytokine cytokine receptor interaction	Up	<0.0001	168	http://www.broadinstitute.org/gsea/msigdb/cards/KEGG_CYTOKINE_CYTOKINE_RECEPTOR_INTERACTION
K11	KEGG ECM receptor interaction	Up	<0.0001	73	http://www.broadinstitute.org/gsea/msigdb/cards/KEGG_ECM_RECEPTOR_INTERACTION
K12	KEGG focal adhesion	Up	0.0009	178	http://www.broadinstitute.org/gsea/msigdb/cards/KEGG_FOCAL_ADHESION
K13	KEGG graft versus host disease	Up	0.0009	25	http://www.broadinstitute.org/gsea/msigdb/cards/KEGG_GRAFT_VERSUS_HOST_DISEASE
K14	KEGG hematopoietic cell lineage	Up	<0.0001	63	http://www.broadinstitute.org/gsea/msigdb/cards/KEGG_HEMATOPOIETIC_CELL_LINEAGE
K15	KEGG intestinal immune network for IgA production	Up	0.0002	32	http://www.broadinstitute.org/gsea/msigdb/cards/KEGG_INTESTINAL_IMMUNE_NETWORK_FOR_IGA_PRODUCTION
K16	KEGG leishmania infection	Up	<0.0001	63	http://www.broadinstitute.org/gsea/msigdb/cards/KEGG_LEISHMANIA_INFECTION
K17	KEGG leukocyte transendothelial migration	Up	0.0049	99	http://www.broadinstitute.org/gsea/msigdb/cards/KEGG_LEUKOCYTE_TRANSENDOTHELIAL_MIGRATION
K18	KEGG natural killer cell mediated cytotoxicity	Up	0.0009	91	http://www.broadinstitute.org/gsea/msigdb/cards/KEGG_NATURAL_KILLER_CELL_MEDIATED_CYTOTOXICITY
K19	KEGG primary immunodeficiency	Up	0.001	26	http://www.broadinstitute.org/gsea/msigdb/cards/KEGG_PRIMARY_IMMUNODEFICIENCY
K20	KEGG systemic lupus erythematosus	Up	0.0015	71	http://www.broadinstitute.org/gsea/msigdb/cards/KEGG_SYSTEMIC_LUPUS_ERYTHEMATOSUS
K21	KEGG TGF beta signaling pathway	Up	0.0015	75	http://www.broadinstitute.org/gsea/msigdb/cards/KEGG_TGF_BETA_SIGNALING_PATHWAY
K22	KEGG toll like receptor signaling pathway	Up	0.0036	81	http://www.broadinstitute.org/gsea/msigdb/cards/KEGG_TOLL_LIKE_RECEPTOR_SIGNALING_PATHWAY
K23	KEGG type I diabetes mellitus	Up	0.0024	29	http://www.broadinstitute.org/gsea/msigdb/cards/KEGG_TYPE_I_DIABETES_MELLITUS
K24	KEGG viral myocarditis	Up	0.0021	57	http://www.broadinstitute.org/gsea/msigdb/cards/KEGG_VIRAL_MYOCARDITIS
R1	Reactome respiratory electron transport	down	<0.0001	63	http://www.broadinstitute.org/gsea/msigdb/cards/REACTOME_RESPIRATORY_ELECTRON_TRANSPORT
R2	Reactome respiratory electron transport ATP synthesis by chemiosmotic coupling and heat production by uncoupling proteins	down	<0.0001	78	http://www.broadinstitute.org/gsea/msigdb/cards/REACTOME_RESPIRATORY_ELECTRON_TRANSPORT_ATP_SYNTHESIS_BY_CHEMIOSMOTIC_COUPLING_AND_HEAT_PRODUCTION_BY_UNCOUPLING_PROTEINS_
R3	Reactome TCA cycle and respiratory electron transport	down	0.0006	114	http://www.broadinstitute.org/gsea/msigdb/cards/REACTOME_TCA_CYCLE_AND_RESPIRATORY_ELECTRON_TRANSPORT
R4	Reactome cell surface interactions at the vascular wall	Up	0.001	78	http://www.broadinstitute.org/gsea/msigdb/cards/REACTOME_CELL_SURFACE_INTERACTIONS_AT_THE_VASCULAR_WALL
R5	Reactome chemokine receptors bind chemokines	Up	<0.0001	40	http://www.broadinstitute.org/gsea/msigdb/cards/REACTOME_CHEMOKINE_RECEPTORS_BIND_CHEMOKINES
R6	Reactome class A1 rhodopsin like receptors	Up	0.0021	141	http://www.broadinstitute.org/gsea/msigdb/cards/REACTOME_CLASS_A1_RHODOPSIN_LIKE_RECEPTORS
R7	Reactome collagen formation	Up	0.0024	49	http://www.broadinstitute.org/gsea/msigdb/cards/REACTOME_COLLAGEN_FORMATION
R8	Reactome costimulation by the CD28 family	Up	0.0034	56	http://www.broadinstitute.org/gsea/msigdb/cards/REACTOME_COSTIMULATION_BY_THE_CD28_FAMILY
R9	Reactome cytokine signaling in immune system	Up	<0.0001	233	http://www.broadinstitute.org/gsea/msigdb/cards/REACTOME_CYTOKINE_SIGNALING_IN_IMMUNE_SYSTEM
R10	Reactome downstream TCR signaling	Up	0.0062	32	http://www.broadinstitute.org/gsea/msigdb/cards/REACTOME_DOWNSTREAM_TCR_SIGNALING
R11	Reactome extracellular matrix organization	Up	0.0002	66	http://www.broadinstitute.org/gsea/msigdb/cards/REACTOME_EXTRACELLULAR_MATRIX_ORGANIZATION
R12	Reactome generation of second messenger molecules	Up	<0.0001	24	http://www.broadinstitute.org/gsea/msigdb/cards/REACTOME_GENERATION_OF_SECOND_MESSENGER_MOLECULES
R13	Reactome gpcr ligand binding	Up	0.0097	200	http://www.broadinstitute.org/gsea/msigdb/cards/REACTOME_GPCR_LIGAND_BINDING
R14	Reactome GPVI mediated activation cascade	Up	0.0087	30	http://www.broadinstitute.org/gsea/msigdb/cards/REACTOME_GPVI_MEDIATED_ACTIVATION_CASCADE
R15	Reactome immunoregulatory interactions between a lymphoid and a non-lymphoid cel	Up	<0.0001	45	http://www.broadinstitute.org/gsea/msigdb/cards/REACTOME_IMMUNOREGULATORY_INTERACTIONS_BETWEEN_A_LYMPHOID_AND_A_NON_LYMPHOID_CELL
R16	Reactome innate immune system	Up	0.0021	194	http://www.broadinstitute.org/gsea/msigdb/cards/REACTOME_INNATE_IMMUNE_SYSTEM
R17	Reactome integrin cell surface interactions	Up	<0.0001	74	http://www.broadinstitute.org/gsea/msigdb/cards/REACTOME_INTEGRIN_CELL_SURFACE_INTERACTIONS
R18	Reactome interferon alpha beta signaling	Up	0.0008	48	http://www.broadinstitute.org/gsea/msigdb/cards/REACTOME_INTERFERON_ALPHA_BETA_SIGNALING
R19	Reactome interferon gamma signaling	Up	0.0009	55	http://www.broadinstitute.org/gsea/msigdb/cards/REACTOME_INTERFERON_GAMMA_SIGNALING
R20	Reactome interferon signaling	Up	0.0001	136	http://www.broadinstitute.org/gsea/msigdb/cards/REACTOME_INTERFERON_SIGNALING
R21	Reactome PD1 signaling	Up	0.001	17	http://www.broadinstitute.org/gsea/msigdb/cards/REACTOME_PD1_SIGNALING
R22	Reactome peptide ligand binding receptors	Up	0.002	91	http://www.broadinstitute.org/gsea/msigdb/cards/REACTOME_PEPTIDE_LIGAND_BINDING_RECEPTORS
R23	Reactome phosphorylation of CD3 and TCR zeta chains	Up	0.0001	15	http://www.broadinstitute.org/gsea/msigdb/cards/REACTOME_PHOSPHORYLATION_OF_CD3_AND_TCR_ZETA_CHAINS
R24	Reactome signaling by ILS	Up	0.001	97	http://www.broadinstitute.org/gsea/msigdb/cards/REACTOME_SIGNALING_BY_ILS
R25	Reactome TCR signaling	Up	<0.0001	47	http://www.broadinstitute.org/gsea/msigdb/cards/REACTOME_TCR_SIGNALING
R26	Reactome toll receptor cascades	Up	0.0042	108	http://www.broadinstitute.org/gsea/msigdb/cards/REACTOME_TOLL_RECEPTOR_CASCADES

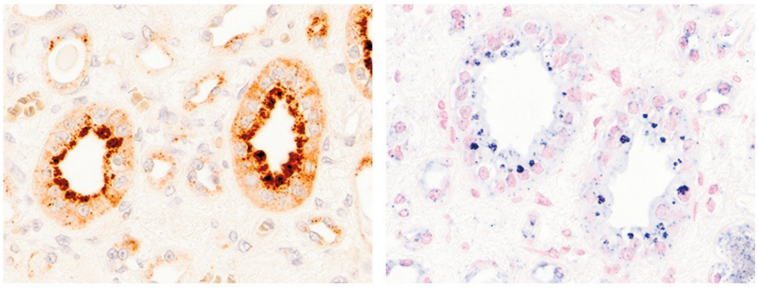

Supplementary Figure S1. Expression of renin (left; red staining) and miR-181a (right; blue staining) in the distal collecting duct. Staining is predominant within the luminal pole of the epithelial cells of the collecting duct (magnification, 400×).

tive staining (renin) was brown, while the counterstain was haematoxylin (blue staining). For ISH, the positive staining was blue while the counterstain was nuclear fast red (red staining). Both ISH and immunohistochemistry were conducted by Bioneer A/S (Denmark). Images were acquired directly from the slides by digital photography using a Nikon Eclipse E800 microscope with 100x, 200x and 400x magnification.

Biochemical Analysis

Serum renin levels were measured by immunoradiometric assay (Renin III, Cisbio, Gif-sur-Yvette) in 192 TRANSLATE subjects from whom both serum sample and kidney tissue samples were available.

Statistical Analysis

In the TRANSLATE Study, distributions of all mRNA expression measurements and biochemical data were examined using the Skewness and Kurtosis test prior to further analysis. Serum renin was non-normally distributed, and was therefore logarithmically transformed to achieve a normal distribution. Unadjusted association analysis between two quantitative phenotypes was explored first by Pearson's linear correlation. Further analyses were conducted using step-wise multiple linear regression models with clinical (age, sex, body mass index, recruitment centre) and experimental (cDNA or qPCR plate) variables as independent parameters (criteria of F-entry probability: 0.15, removal: 0.20). Additional biochemical (serum levels of renin) or molecular (renal expression of renin mRNA) parameters were included in the models where appropriate. Three types of sensitivity analysis were used after analysis of association between gene expression or biochemical phenotypes and BP values. In the first type of sensitivity analysis, BP from patients receiving antihypertensive medication were corrected for the BP lowering effect of medications by adding a constant of 15 mmHg and 10 mmHg to the systolic BP (SBP) and diastolic BP (DBP) measurements, respectively, in line with the algorithms used before (14). The second sensitivity analysis was based on exclusion of all subjects on antihypertensive therapy. The third sensitivity analysis included only individuals with clinic SBP ≤ 140 mmHg and DBP ≤ 90 mmHg, who were not taking antihypertensive medication.

In the GRAPHIC Study, data were first checked to ensure that assumptions for multiple regression analyses were met. Multiple linear regression analyses were performed using clinic SBP or clinic DBP as the dependent variable and miR-181a dCt, age, body mass index and sex as independent variables.

Results obtained at the $P < 0.05$ level were considered statistically significant. Statistical package SPSS for Windows (Release 21.0 for TRANSLATE and 20.0 for GRAPHIC) was used for the statistical analyses.

Pathway Analysis of Human Kidney Transcriptomes Characterized by Next-Generation RNA-Sequencing

Next-generation RNA-sequencing and small RNA-sequencing raw data (level 1) from kidney tissue unaffected by cancer (labeled as "normal–matched") collected from 69 individuals with clear cell renal carcinoma were downloaded from The Cancer Genome Atlas (TCGA) database (http://tcga-data.nci.nih.gov) in April 2014 (application 26966-1 approved by TCGA Data Access Committee). Raw 50 base pair reads were first aligned to the GRCh37 reference genome (as used by Ensembl release 70) using the TopHat programme (15). On average, 68 million paired-end reads per sample were aligned successfully. Expression values were calculated for all Ensembl transcripts and genes using Cufflinks and Cuffdiff software (16). The final expression values were computed in $\log_2$TPM+1 (TPM: transcripts per million) units as described in previous studies (17, 18). Technical variation between the samples was accounted for by normalization based on probabilistic estimation of expression residuals (PEER) (19, 20). Analysis of association between miR-181a and mRNAs was conducted using Limma (21), with each mRNA expression value as the response variable and miR-181a expression, age and sex as independent parameters included in the regression model.

To identify renal pathways associated with expression of miR-181a, we used gene-set enrichment analysis (22) (in pre-ranked mode) with Kyoto Encyclopedia of Genes and Genomes (KEGG), BioCarta and Reactome as pathway repositories. The t-statistics generated were averaged by gene. The pathway overlap, and therefore edge width, was calculated using the overlap coefficient. The resultant pathway network was visualized using Gephi (23) and annotated manually to highlight clusters of pathways with similar functions. Correction for multiple testing in both individual mRNA- and pathway-based analyses was conducted by calculation of false discovery rate q-values and the cor-

rected threshold for statistical significance was set at $q < 0.01$.

Hierarchical Clustering of Multidimensional Scaling of Renal Transcriptomes Characterized by Next-Generation RNA-Sequencing

To exclude the potential effect of co-existent cancer on the transcriptome of the tumour-unaffected renal tissue from where the specimen was sampled, we compared global expression profiles of healthy tissue from nephrectomies due to cancer with those from non-cancer kidneys and clear cell renal carcinoma. The RNA-sequencing data were collected from three sources: TCGA (69 normal-matched and 10 randomly chosen renal cancer samples), Genotype-Tissue Expression (GTEx) Project (24) (8 non-cancer kidneys harvested from donors identified through low post-mortem interval) and TRANSLATE P Study (where 32 kidneys underwent next-generation RNA-sequencing).

RNA-sequencing sample preparation and quality control – TRANSLATE Study. Approximately 30 milligrams of tissue was mechanically homogenized (PowerGen™ Model 125 Homogenizer) in Qiagen RTL buffer. RNA extraction was conducted using RNeasy Mini kit (Qiagen) according to the supplier's guidelines. Eluted RNA samples were assessed for concentration using a Nanodrop 8-sample spectrophotometer ND-800 prior to further processing. RNA sequencing libraries were prepared using a non-strand-specific Illumina TruSeq v2 kit and 1 μg of poly-A selected input RNA at the Australian Genome Research Facility (AGRF). Libraries were sequenced on an Illumina HiSeq 2000 using 100 base pair paired-end reads, producing an average of ~52 million reads per sample. Raw reads were checked for quality using FastQC (http://www.bioinformatics.babraham.ac.uk/projects/fastqc/). Post-alignment, the squared coefficient of variation and expression dispersion estimates were assessed using CummeRBund (25).

RNA-sequencing data processing – GTEx Project. GTEx samples were pre-

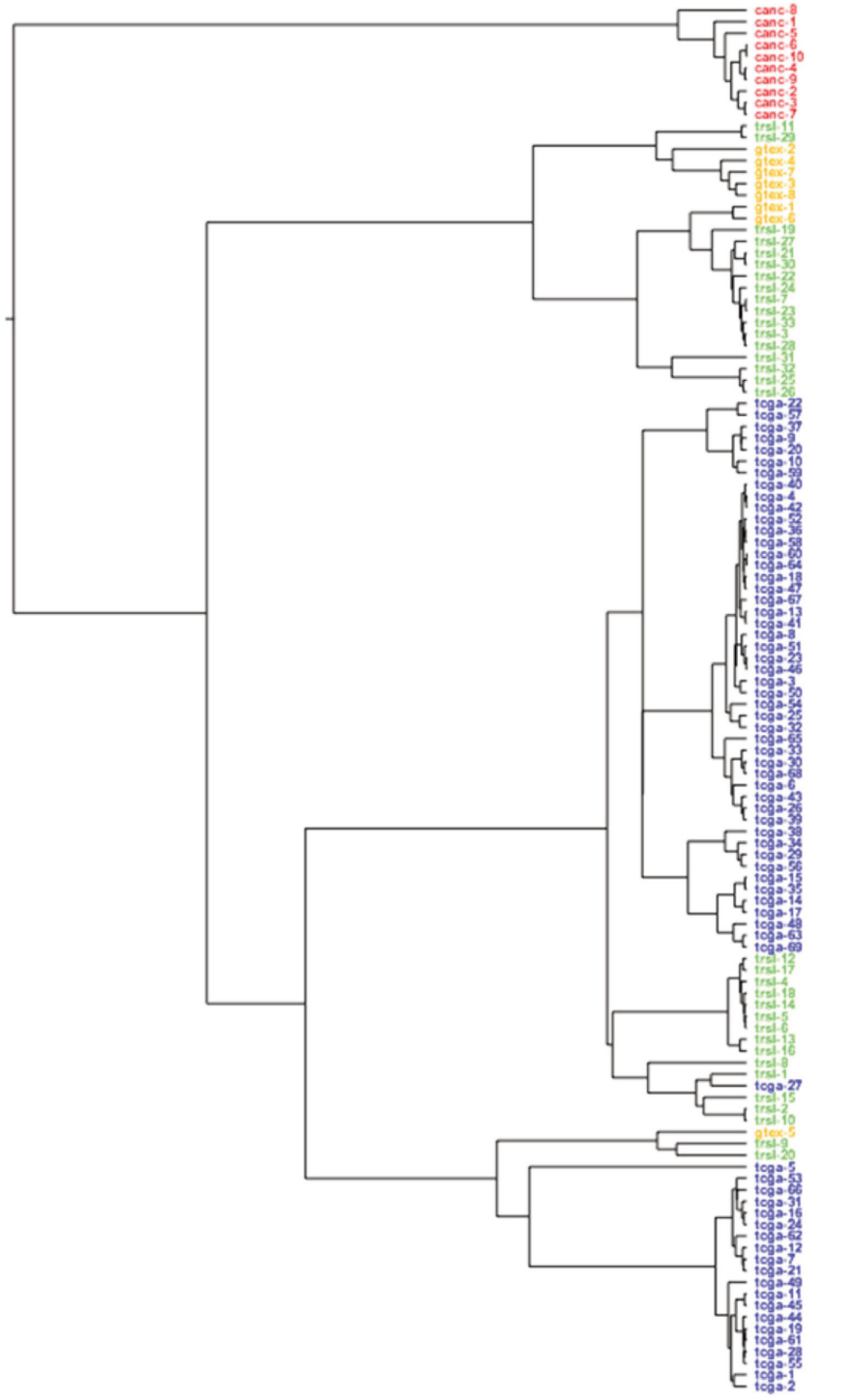

Supplementary Figure S2. Hierarchical clustering of renal transcriptomes characterized by next-generation RNA-sequencing. The expression values for 12551 commonly expressed mRNAs were represented in three dimensions via classical multidimensional scaling (MDS) and then clustered into a hierarchical structure from a pairwise Euclidean distance matrix. The horizontal axis represents Euclidean distance between samples in the three MDS dimensions. Blue, the Cancer Genome Atlas (TCGA) "normal-matched" samples; green, TRANSLATE samples from tissue unaffected by cancer; orange, Genotype-Tissue Expression (GTEx) non-cancer renal samples; red, TCGA renal cancer samples.

pared and sequenced using a protocol very similar to the TRANSLATE Study. All libraries were poly-A selected and non-strand specific and were sequenced on an Illumina HiSeq 2000 using 76 bp paired-end reads giving approximately 50 million reads per sample. The latest details of the GTEx data and their analysis methods can be found in their online documentation (http://www.gtexportal.org/home/documentationPage) and in the published literature (24, 26).

Data processing and multidimensional scaling analysis. Expression values were calculated as $\log_2$ read counts per million (CPM) for all genes expressed above 20 CPM in more than 50% of samples from any group. Read counts were provided by Cufflinks (16) except for the GTEx samples, which were downloaded from the GTEx portal (http://www.gtexportal.org/home/). Normalization, CPM calculation and multidimensional scaling of the data into three dimensions was performed by edgeR (27). Hierarchical clustering of multidimensional scaling dimension values and distance matrix calculation was performed by R (28) and visualized using FigTree v1.4.2 (29).

REFERENCES

1. Tomaszewski M, Eales J, Denniff M, Myers S, Chew GS, Nelson CP, *et al*. (2015) Renal mechanisms of association between FGF1 and blood pressure. *J Am Soc Nephrol*. Published Online First: 27th April, 2015; doi: 10.1681/ASN.2014121211
2. Tomaszewski M, Charchar FJ, Lynch MD, Padmanabhan S, Wang WY, Miller WH, *et al*. (2007) Fibroblast growth factor 1 gene and hypertension: from the quantitative trait locus to positional analysis. *Circulation*. 116:1915-24.
3. Tomaszewski M, Charchar FJ, Nelson CP, Barnes T, Denniff M, Kaiser M, *et al*. (2011) Pathway analysis shows association between FGFBP1 and hypertension. *J Am Soc Nephrol*. 22:947-55.
4. Tomaszewski M, Brain NJ, Charchar FJ, Wang WY, Lacka B, Padmanabahn S, *et al*. (2002) Essential hypertension and β_2-adrenergic receptor gene: linkage and association analysis. *Hypertension*. 40:286-91.
5. Tomaszewski M, Charchar FJ, Lacka B, Pesonen U, Wang WY, Zukowska-Szczechowska E, *et al*. (2004) Epistatic interaction between β2-adrenergic receptor and neuropeptide Y genes influences LDL-cholesterol in hypertension. *Hypertension*. 44:689-94.
6. Tobin MD, Tomaszewski M, Braund PS, Hajat C, Raleigh SM, Palmer TM, *et al*. (2008) Common variants in genes underlying monogenic hypertension and hypotension and blood pressure in the general population. *Hypertension*. 51:1658-64.
7. Tomaszewski M, Debiec R, Braund PS, Nelson CP, Hardwick R, Christofidou P, *et al*. (2010) Genetic architecture of ambulatory blood pressure in the general population: insights from cardiovascular gene-centric array. *Hypertension*. 56:1069-76.
8. Marques FZ, Campain AE, Tomaszewski M, Zukowska-Szczechowska E, Yang YH, Charchar FJ, *et al*. (2011) Gene expression profiling reveals renin mRNA overexpression in human hypertensive kidneys and a role for microRNAs. *Hypertension*. 58:1093-8.
9. Lorenzen JM, Thum T. (2012) Circulating and urinary microRNAs in kidney disease. *Clin J Am Soc Nephrol*. 7:1528-33.
10. Brase JC, Wuttig D, Kuner R, Sultmann H. (2010) Serum microRNAs as non-invasive biomarkers for cancer. *Mol Cancer*. 9:306.
11. Kuner R, Brase JC, Sultmann H, Wuttig D. (2013) microRNA biomarkers in body fluids of prostate cancer patients. *Methods*. 59:132-7.
12. Li Y, Kowdley KV. (2012) Method for microRNA isolation from clinical serum samples. *Anal Biochem*. 431:69-75.
13. Schmittgen TD, Livak KJ. (2008) Analyzing real-time PCR data by the comparative C_T method. *Nat Protoc*. 3:1101-8.
14. Ehret GB, Caulfield MJ. (2013) Genes for blood pressure: an opportunity to understand hypertension. *Eur Heart J*. 34:951-61.
15. Kim D, Pertea G, Trapnell C, Pimentel H, Kelley R, Salzberg SL. (2013) TopHat2: accurate alignment of transcriptomes in the presence of insertions, deletions and gene fusions. *Genome Biol*. 14:R36.
16. Trapnell C, Hendrickson DG, Sauvageau M, Goff L, Rinn JL, Pachter L. (2013) Differential analysis of gene regulation at transcript resolution with RNA-seq. *Nat Biotechnol*. 31:46-53.
17. Li B, Dewey CN. (2011) RSEM: accurate transcript quantification from RNA-Seq data with or without a reference genome. *BMC Bioinformatics*. 12:323.
18. Li B, Ruotti V, Stewart RM, Thomson JA, Dewey CN. (2010) RNA-Seq gene expression estimation with read mapping uncertainty. *Bioinformatics*. 26:493-500.
19. Hoen PA, Friedlander MR, Almlof J, Sammeth M, Pulyakhina I, Anvar SY, *et al*. (2013) Reproducibility of high-throughput mRNA and small RNA sequencing across laboratories. *Nat Biotechnol*. 31:1015-22.
20. Stegle O, Parts L, Piipari M, Winn J, Durbin R. (2012) Using probabilistic estimation of expression residuals (PEER) to obtain increased power and interpretability of gene expression analyses. *Nat Protoc*. 7:500-7.
21. Smyth GK. (c2005) limma: Linear Models for Microarray Data. In: *Bioinformatics and Computational Biology Solutions Using R and Bioconductor*. Gentleman R, Carey VJ, Huber W, Irizarry RA, Dudoit S (eds.) Springer, New York, pp. 397–420.
22. Subramanian A, Tamayo P, Mootha VK, Mukherjee S, Ebert BL, Gillette MA, *et al*. (2005) Gene set enrichment analysis: a knowledge-based approach for interpreting genome-wide expression profiles. *Proc Natl Acad Sci USA*. 102:15545-50.
23. Bastian M, Heymann S, Jacomy M, editors. Gephi : an open source software for explorating and manipulating networks. International AAAI Conference on Weblogs and Social Media; 2009.
24. Lonsdale J, Thomas J, Salvatore M, Phillips R, Lo E, Shad S, *et al*. (2013) The Genotype-Tissue Expression (GTEx) project. *Nat Genet*. 45:580-5.
25. Goff L, Trapnell C, Kelley D. CummeRbund: visualization and exploration of Cufflinks high-throughput sequencing data.: R package version 2.6.1.; 2012.
26. DeLuca DS, Levin JZ, Sivachenko A, Fennell T, Nazaire MD, Williams C, *et al*. (2012) RNA-SeQC: RNA-seq metrics for quality control and process optimization. *Bioinformatics*. 28:1530-2.
27. Robinson MD, McCarthy DJ, Smyth GK. (2010) edgeR: a Bioconductor package for differential expression analysis of digital gene expression data. *Bioinformatics*. 26:139-40.
28. R Core Team. (2014) R: A Language and Environment for Statistical Computing. Available: http://www.R-project.org.
29. Rambaut A. (2014) FigTree v1.4.2. Available: http://tree.bio.ed.ac.uk/software/figtree.